ELSEVIER

Journal of Nuclear Materials 266–269 (1999) 862–866

journal of nuclear materials

Measured and simulated poloidal asymmetries of the FTU SOL in the toroidal limiter configuration

M. Leigheb [a,*], V. Pericoli Ridolfini [a], R. Zagorski [b]

[a] *Associazione EURATOM-ENEA sulla Fusione, Centro Ricerche Energia, C.P. 65, 00044 Frascati, Rome, Italy*
[b] *Institute of Plasma Physics and Laser Microfusion, Warsaw, Poland*

Abstract

The scrape-off layer (SOL) of FTU in the magnetic configuration generated by a TZM (Molybdenum) toroidal limiter has been studied by an array of reciprocating Langmuir probes extended over a large part of the poloidal angle, and the results have been compared with the 2-dimensional multifluid SOL code EPIT. A comparison with the previous poloidal limiter configuration with the same main plasma conditions, showed at the last closed magnetic surface (LCMS) longer and more poloidally uniform connection lengths, and a corresponding better uniformity of SOL plasma parameters. Asymmetry of electron density is observed, which can be associated with the recycling of plasma near the toroidal limiter plates in a configuration with long connection lengths. Electron temperature appears to be less dependent of power entering the SOL than in the old poloidal limiter configuration. Experimentally observed dependence of the edge plasma condition on L_{con} has been confirmed by the results of the 2D code EPIT.

Keywords: 2D measurements; FTU; Langmuir probe; SOL modeling

1. Introduction

Strong poloidal asymmetries were already observed on FTU, and their cause was previously proposed to be the poloidal variation of the magnetic connection length L_{con} [1]. This variation is expected in a poloidal limiter tokamak when the LCMS does not match exactly the limiter and is further exalted if the limiter is not poloidally continuous (as in FTU until 1994), where a field line close to LCMS may travel several toroidal turns before hitting the limiter.

With the toroidal limiter now operating on FTU, a different behaviour of electron temperature and density is found. The connection lengths are longer and the poloidal uniformity of SOL plasma parameters is better. Nevertheless, residual poloidal asymmetry is still observed, and higher values of electron density are measured by probes near to the limiter; this effect is associated to longer connection lengths, lower particle fluxes into the SOL and high recycling conditions.

To study with more accuracy the effect of the magnetic configuration on SOL parameters, we compare discharges in the magnetic configuration generated by the poloidal limiter with similar discharges in the magnetic configuration generated by the toroidal limiter now operating on FTU. The experimental results are simulated with the 2-dimensional multifluid SOL code EPIT [2].

2. Experimental set-up

FTU is a high toroidal field tokamak [3] ($R = 0.935$ m, $a = 0.295$ m, $B_T = 3.8$–7.1 T) characterized by an average high ohmic power density (>1.5 MW/m^3) and a wide range of main plasma parameters ($\langle n_e \rangle = 0.2 \times 10^{20}$–$2 \times 10^{20}$ m^{-3} for the line averaged density, and $I_p = 0.3$–1.0 MA for the plasma current). Additional radio frequency plasma heating is possible.

* Corresponding author. Tel.: +39-06 9400 5431; fax: +39-06 9400 5735; e-mail: leigheb@frascati.enea.it.

0022-3115/99/$ – see front matter
PII: S0022-3115(98)00553-4

The original magnetic configuration, that operated until 1994, was generated by three Inconel poloidal limiters located at a radius 0.3 m, the first (at the inner side of the vessel) with a poloidal extension of 148°, the second (at the outer side in the same toroidal position of the first) with a poloidal extension of 87°, and the third equal to the second but 150° toroidally away. Since 1996 an inner toroidal TZM (Molybdenum) limiter of 0.29 m radius has been operating [4], and a single Inconel poloidal limiter was added occasionally.

To study the behaviour of the SOL at the LCMS in the different magnetic configurations without affecting the bulk, in the present analysis we are examining ohmic discharges at $B_T = 6$ T and with similar main plasma parameters in three different regimes: low plasma current ($I_p = 0.5$ MA) and low electron density ($\langle n_e \rangle = 0.6-0.8 \times 10^{20}$ m^{-3}), high plasma current ($I_p = 0.8$ MA) and low electron density ($\langle n_e \rangle = 0.8 \times 10^{20}$ m^{-3}), high plasma current ($I_p = 0.8$ MA) and high electron density ($\langle n_e \rangle = 1.3$–$1.5 \times 10^{20}$ m^{-3}).

The magnetic surfaces, the position of the last closed magnetic surface (LCMS) and the values of the connection length L_{con} at the LCMS are derived by the equilibrium reconstruction. Electron density $n_e(r)$ and temperature $T_e(r)$ are measured by an array of reciprocating Langmuir probes extended over a large part of the poloidal angle. For each probe, $n_e(r)$ and $T_e(r)$ are derived by a complete fit of the I (collected current) vs. V (applied voltage) characteristic, repeated at a frequency $\upsilon = 500$ Hz. Whenever the probe does not reach the LCMS, the values of T_e, n_e and the corresponding decay lengths are extrapolated assuming an exponential trend along the SOL [1,5]. T_e and n_e decay lengths are divided by $(L_{con}/\pi R)^{1/2}$ to be free from first order geometrical effects [6].

3. Numerical model description

The 2-dimensional edge plasma code EPIT [2] has been used to simulate experimental results. The model describes the electrons and various ion species in their different charge states as separate fluids [7]. The transport along field lines is assumed to be classical [8], whereas the radial transport is anomalous with constant radial transport coefficients. For every ion species the continuity and the momentum equations are solved together with two equations for the plasma temperature. Equations of different fluids are coupled by electrostatic, friction and thermal forces as well as by atomic processes. The model accounts for curvilinear geometry of the magnetic surfaces in the FTU tokamak, assuming the Shafranov shift $\Delta = 4$ cm and the toroidal TZM limiter in the $\theta = 180°$ position but for simplicity we do not consider the real structure of the toroidal limiter. The dynamic of hydrogen and impurity neutrals in the SOL is described by an analytical model, which accounts in a self-consistent way for recycling of plasma ions as well as sputtering processes at the limiter plates [2].

4. Investigation of the poloidal asymmetries

As already reported [6], the poloidal magnetic configuration had shorter and non-poloidally uniform connection lengths at the LCMS, corresponding to a poloidal non-uniformity of electron density and temperature at LCMS. On the contrary, in the toroidal magnetic configuration L_{con} at the LCMS is more uniform poloidally, and this corresponds to a better poloidal uniformity of electron density and temperature at LCMS. When the low current, toroidal limiter configuration is considered, longer connection lengths are found, and higher density values for probes situated near the toroidal limiter are detected. In Fig. 1 the values of total connection length L_{con} at the LCMS vs. poloidal angle (as calculated by equilibrium reconstruction) are indicated for both the poloidal and toroidal configurations in the three different plasma regimes.

According to the EPIT code, longer connection lengths together with high plasma density in the SOL are responsible for large density poloidal asymmetries in cases of high recycling (complex SOL). On the contrary, in conditions of low recycling the same values of plasma parameters are more uniform poloidally.

5. Dependence of SOL quantities on plasma parameters

The influence of central line averaged electron density $\langle n_e \rangle$ and L_{con} on average SOL quantities, particularly on n_e(LCMS), is confirmed by comparison with the linear regression already found for FTU [6].

$$n_e(\mathrm{LCMS}) \propto 2.46 \times 10^{-9} (\langle n_e \rangle / f_{pk})^{1.36} L_{con}^{96}, \quad (1)$$

where $f_{pk} = n_e(0)/\langle n_e \rangle$ is the density peaking factor. The direct dependence of n_e(LCMS) on the connection length L_{con} (already explained by a simple 1D model [9] and experimentally verified [6] on FTU) is still found but lower average values of n_e(LCMS) in the toroidal limiter configuration are measured (Fig. 2).

The dependence of T_e(LCMS) on L_{con} changes with the magnetic configuration and the regime considered (Fig. 3). At low plasma current and low electron density T_e(LCMS) appears almost independent on L_{con} both in the poloidal and in the toroidal configuration. At high plasma current, and particularly at high electron density, a direct dependence is evident, but this dependence appears weaker in the toroidal configuration.

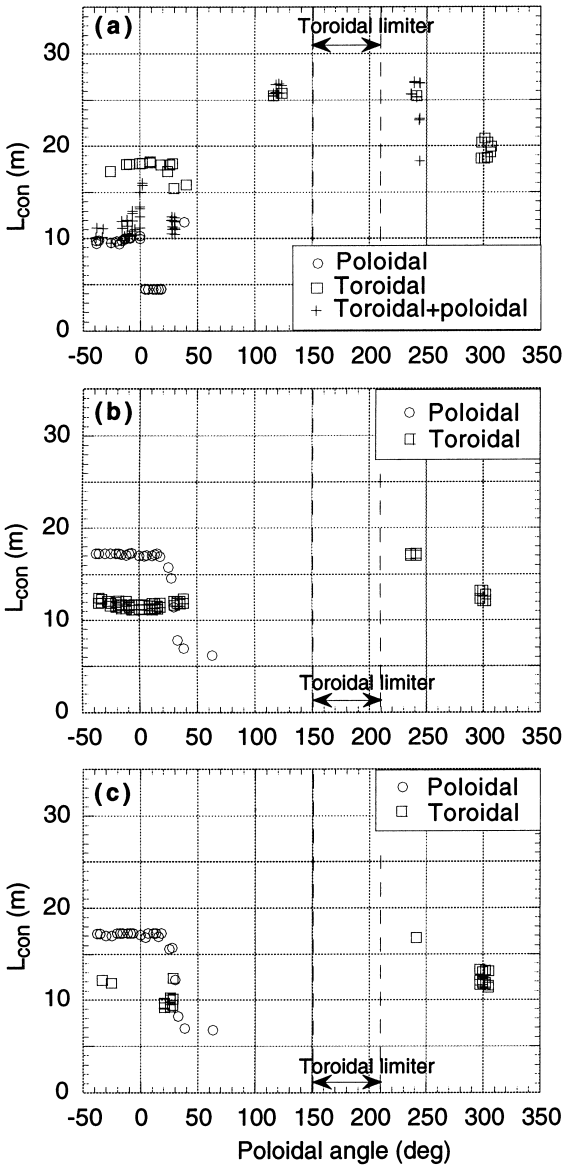

Fig. 1. Total connection length at LCMS vs. poloidal angle in the poloidal (circles), toroidal (squares) and toroidal + poloidal (crosses) configuration; (a) $I_p = 0.5$ MA; (b) $I_p = 0.8$ MA, $\langle n_e \rangle = 0.8 \times 10^{20}$ m^{-3}; (c) $I_p = 0.8$ MA, $\langle n_e \rangle = 1.3 \times 10^{20}$–$1.5 \times 10^{20}$ m^{-3}.

6. Discharges at $I_p = 0.5$ MA

These discharges have $\langle n_e \rangle = 0.6 \times 10^{20}$–$0.8 \times 10^{20}$ m^{-3} as line averaged density, $I_p = 0.5$ MA as plasma current, $T_e = 1.5$–2.0 keV as central electron temperature, $Z_{eff} \approx 2$ as derived from Bremsstrahlung measurements or Spitzer's resistivity, $P_{ohm} = 0.7$ MW as total ohmic power; a power flux into the SOL $P_{SOL} \approx 0.2$–0.3 MW is estimated from bolometric measurements.

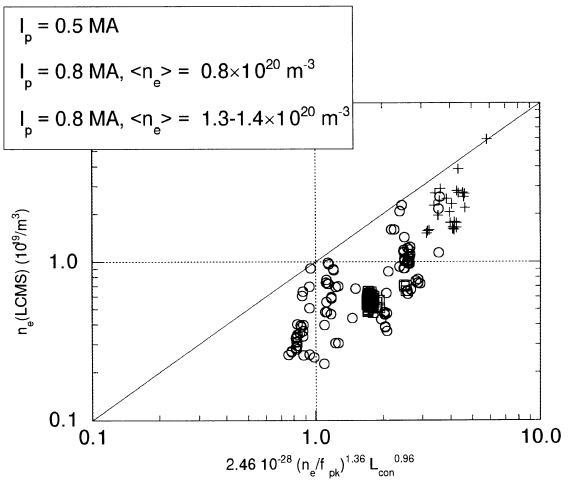

Fig. 2. Comparison of present data with the scaling law already found for FTU in the poloidal configuration; circles: $I_p = 0.5$ MA, squares: $I_p = 0.8$ MA, $\langle n_e \rangle = 0.8 \times 10^{20}$ m^{-3}; crosses: $I_p = 0.8$ MA, $\langle n_e \rangle = 1.3 \times 10^{20}$–$1.5 \times 10^{20}$ m^{-3}.

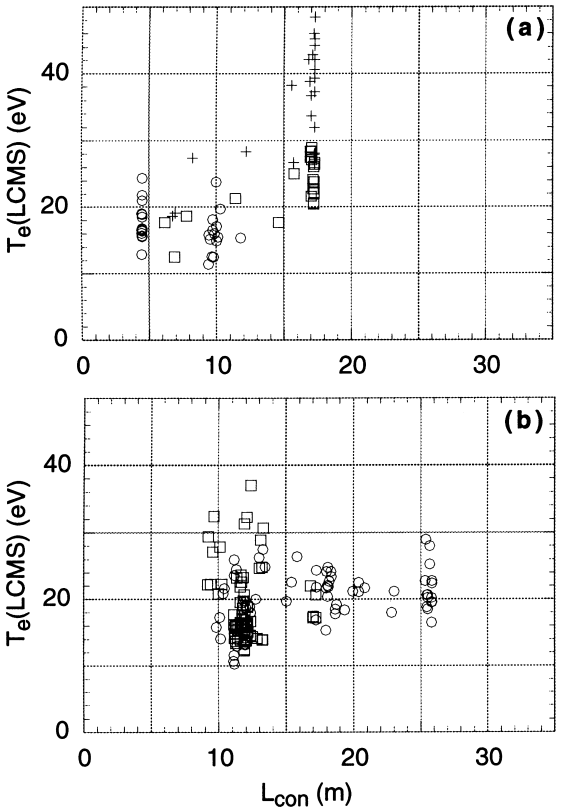

Fig. 3. T_e(LCMS) vs. L_{con}; circles: $I_p = 0.5$ MA; squares: $I_p = 0.8$ MA, $\langle n_e \rangle = 0.8 \times 10^{20}$ m^{-3}; crosses: $I_p = 0.8$ MA, $\langle n_e \rangle = 1.3 \times 10^{20}$–$1.5 \times 10^{20}$ m^{-3}; (a) poloidal configuration; (b) toroidal configuration.

The difference between the connection lengths at the LCMS in the old poloidal magnetic configuration and the new toroidal configuration is very strong (Fig. 1(a)). In the poloidal configuration we find 4 m $< L_{con} <$ 13 m, and this variation is associated with similar variations of electron temperature and density at the LCMS: 12 eV $< T_e$(LCMS) $<$ 24 eV and 1.3×10^{19} m^{-3} $< n_e$(LCMS) $< 3 \times 10^{19}$ m^{-3}.

In the toroidal configuration we find poloidally uniform values for probes poloidally far from the limiter: $L_{con} = 18$ m, $n_e(\text{LCMS}) \approx 1.2 \times 10^{19}\text{m}^{-3}$ and $T_e(\text{LCMS}) = 22$ eV. On the contrary, for probes near to the limiter, connection lengths and electron densities rise up to $L_{con} = 26$ m and $n_e(\text{LCMS}) \approx 2 \times 10^{19}\text{m}^{-3}$, whereas a low value of $T_e(\text{LCMS}) = 19$ eV is detected. The density decay length is found $\lambda_n \approx 1$ cm in the poloidal configuration and $\lambda_n \approx 1.7$ cm in the toroidal case.

When a second (poloidal) limiter is added to the toroidal one, L_{con} is shorter and the lowest values of $n_e(\text{LCMS}) \approx 0.75 \times 10^{19}\text{m}^{-3}$ are found, in agreement with the scaling law and code results; in this case L_{con} is poloidally nonuniform (as in the old poloidal configuration), and the same is also true for n_e(LCMS) and T_e(LCMS).

The average values of n_e(LCMS) in the toroidal configuration are lower than those expected from comparison with the scaling law already found for FTU [6] in the poloidal configuration. This result can be reproduced by the EPIT code only if in the toroidal limiter geometry we assume a lower particle flux from the main plasma into the SOL and a perpendicular electron heat conductivity higher than in the poloidal limiter geometry. In the poloidal case, the best parameters appear to be $\Gamma_{SOL} = 2.4 \times 10^{21}$ s^{-1} as particle flux into the SOL, $P_{SOL} = 0.13$ MW as power flux into the SOL, $R = 0.7$ as recycling factor at the limiter defined as $R = (|\Gamma_{lim}| - |\Gamma_{SOL}|)/|\Gamma_{lim}|$, $D_\perp = 0.3$ m^2 s^{-1} as perpendicular particle diffusion coefficient and $\chi_\perp = 0.9$ m^2 s^{-1} as perpendicular electron heat conductivity. In toroidal case, the best parameters appear to be $R = 0.9$, $\Gamma_{SOL} = 0.39 \times 10^{21}$ s^{-1}, $P_{SOL} = 0.2$ MW, $D_\perp = 0.3$ m^2 s^{-1} and $D_\perp = 7.5$ m^2 s^{-1}.

The experimental increase of electron density measured by the probes poloidally near to the limiter could be explained partly by the increase of connection length and partly by the high recycling near the limiter plate, though it is not possible to discriminate experimentally between the two effects so far. The weak experimental dependence of T_e(LCMS) on L_{con} is explained with two counteracting effects: the low particle flux into the SOL and long L_{con} would lead to an increase of T_e, whereas the higher densities, the enhanced recycling and the onset of parallel-field T_e gradients tend to decrease the temperature in proximity of the limiter.

7. Discharges at $I_p = 0.8$ MA, low density

These discharges have $\langle n_e \rangle = 0.8 \times 10^{20}$ m^{-3}, $I_p = 0.8$ MA, $T_e = 2.0$ keV, $Z_{eff} = 2.0$ as derived from Bremsstrahlung measurements, $P_{ohm} \approx 1.4$ MW and $P_{SOL} \approx 0.3$ MW.

As we have already seen (Fig. 1(b)), L_{con} at the LCMS in the old poloidal magnetic configuration has a variation near the midplane, going from $L_{con} = 6$ m to $L_{con} = 17$ m; on the contrary, in the toroidal limiter configuration we find $L_{con} = 13$ m at all positions with the exception of the probes near to the limiter, where $L_{con} = 17$ m.

The Langmuir probe measurements are shown in Fig. 4 together with the EPIT code simulations. In the poloidal limiter configuration we find $\langle n_e(\text{LCMS}) \rangle \approx 0.71 \times 10^{19}$ m^{-3} and $\langle T_e(\text{LCMS}) \rangle = 23$ eV. In the toroidal limiter configuration, despite the higher values of L_{con}, we find $\langle n_e(\text{LCMS}) \rangle \approx 0.57 \times 10^{19}$ m^{-3} and $\langle T_e(\text{LCMS}) \rangle = 16$ eV, but a little increase of both $n_e(\text{LCMS}) \approx 0.65 \times 10^{19}$ m^{-3} and $T_e(\text{LCMS}) = 18$ eV is detected by the probes poloidally near to the limiter. The

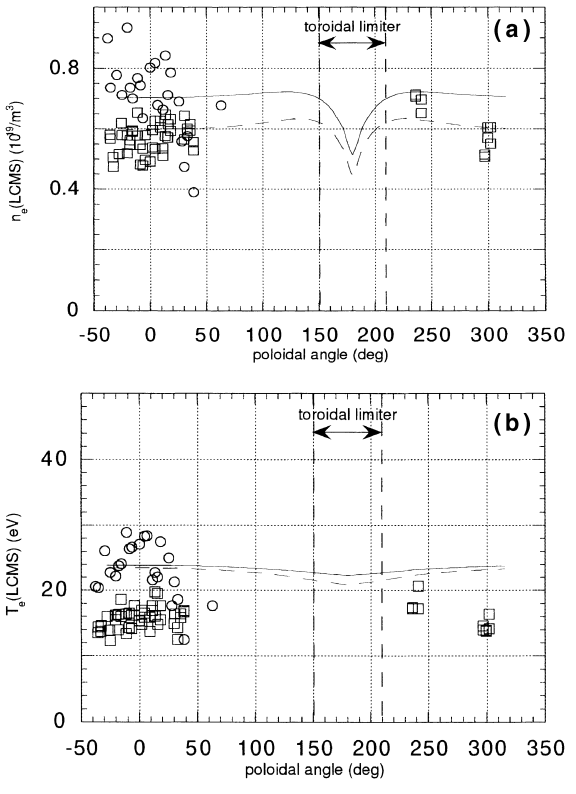

Fig. 4. n_e(LCMS) and T_e(LCMS) vs. poloidal angle at $I_p = 0.8$ MA and $\langle n_e \rangle = 0.8 \times 10^{20}$ m^{-3}; results from EPIT code in the poloidal (solid line) and toroidal (dashed line) configuration; measurements from Langmuir probes in the poloidal (circles) and toroidal (squares) limiter configuration; (a) n_e, (b) T_e.

density decay length is found $\lambda_n \approx 1.2$ cm in the poloidal configuration and $\lambda_n \approx 1.5$ cm in the toroidal one.

By comparing the results with the EPIT code, assuming $R = 0.6$, $\Gamma_{SOL} = 1.6 \times 10^{21}$ s^{-1}, $P_{SOL} = 0.2$ MW, $D_\perp = 0.6$ m^2 s^{-1} and $\chi_\perp = 5.4$ m^2 s^{-1}, we obtain $\langle n_e(\text{LCMS})\rangle \approx 0.7 \times 10^{19}$ m^{-3} and $\langle T_e(\text{LCMS})\rangle \approx 24$ eV, that correspond to the poloidal case.

Regarding the toroidal case we found the best agreement assuming R = 0.8, $\Gamma_{SOL} = 0.6 \times 10^{21}$ s^{-1}, $P_{SOL} = 0.2$ MW, $D_\perp = 0.6$ m^2 s^{-1} and $\chi_\perp = 5.4$ m^2 s^{-1}; with these parameters, we found $\langle n_e(\text{LCMS})\rangle \sim 0.6 \times 10^{19}$ m^{-3} and $\langle T_e(\text{LCMS})\rangle \sim 23$ eV slightly higher than in experiment. In our opinion the discrepancy between the calculated and experimental temperatures is due to the difficulty to simulate the sputtering when the field lines have small angles of incidence with the limiter plates, and should be investigated in a more detailed way (e.g. comparing experimental and calculated fluxes of molybdenum).

8. Discharges at $I_p = 0.8$ MA, high density

These discharges have $\langle n_e\rangle = 1.3 \times 10^{20}$–$1.5 \times 10^{20}$ m^{-3}, $I_p = 0.8$ MA, $T_e = 1.2$–1.5 keV, $Z_{eff} = 1.2$ as derived from Bremsstrahlung measurements, $P_{ohm} \approx 1.3$–1.4 MW and $P_{SOL} \approx 0.4$–0.6 MW.

The non-uniformity of L_{con} at the LCMS in the poloidal magnetic configuration (6 m $< L_{con} <$ 17 m) becomes lower in the toroidal configuration (10 m $< L_{con} <$ 17 m). By comparing this regime with the previous one, we find that the behaviour of electron density at LCMS follows the central electron density, with $\langle n_e(\text{LCMS})\rangle \approx 4 \times 10^{19}$ m^{-3} in the poloidal limiter configuration and $\langle n_e(\text{LCMS})\rangle \approx 2.2 \times 10^{19}$ m^{-3} in the toroidal limiter configuration. On the contrary, dealing with electron temperatures we find high values ($\langle T_e(\text{LCMS})\rangle = 35$ eV) in the poloidal limiter configuration, and lower ($\langle T_e(\text{LCMS})\rangle = 24$ eV) in the toroidal limiter configuration. The SOL depth does not change ($\lambda_n \approx 1.2$ cm).

By comparing the results with the EPIT code, assuming $R = 0.6$, $\Gamma_{SOL} = 9.5 \times 10^{21}$ s^{-1}, $P_{SOL} = 0.6$ MW, $D_\perp = 0.3$ m^2 s^{-1} and $\chi_\perp = 0.9$ m^2 s^{-1}, we obtain $\langle n_e(\text{LCMS})\rangle \approx 3.8 \times 10^{19}$ m^{-3} and $\langle T_e(\text{LCMS})\rangle \approx 30$ eV, that correspond to the poloidal case. To reproduce the toroidal case, it was necessary to assume a lower particle flux from the main plasma into the SOL and a higher perpendicular electron heat conductivity than in the poloidal limiter geometry; the code parameters were $R = 0.8$, $\Gamma_{SOL} = 3.0 \times 10^{21}$ s^{-1}, $P_{SOL} = 0.6$ MW, $D_\perp = 0.6$ m^2 s^{-1} and $\chi_\perp = 9.0$ m^2 s^{-1}, obtaining $\langle n_e(\text{LCMS})\rangle \approx 2.6 \times 10^{19}$ m^{-3} and $\langle T_e(\text{LCMS})\rangle \approx 25$ eV.

9. Conclusion

In the FTU tokamak, the magnetic configuration generated by the new toroidal TZM limiter is associated with more poloidally uniform electron densities, temperatures and connection lengths at LCMS (when compared with the old configuration with an Inconel poloidal limiter), as measured by a set of reciprocating Langmuir probes. Electron densities at LCMS in the toroidal configuration are also lower than ones in the poloidal configuration; this result can be explained by simulations with the 2-dimensional multifluid SOL code EPIT, assuming lower particle fluxes into the SOL associated with lower densities at LCMS and high recycling. Results of calculations indicate also (in agreement with Ref. [6]) that in the toroidal configuration radial heat conductivity is larger than in the poloidal configuration. A possible weaker dependence of electron temperature at LCMS on connection length in the toroidal configuration needs more experimental data to be confirmed.

From experiments and simulation results it is apparent that in the toroidal configuration, in cases with long connection length (shots with $I_p = 0.5$ MA) as well as in high density discharges (high density shots with $I_p = 0.8$ MA), conditions with large parallel field T-gradients in the FTU tokamak SOL are created (in agreement with the results of an independent self-consistent model of FTU in Ref. [10]), leading to the increase of plasma density close to the limiter plates and to the decrease of the plasma temperature. Such conditions, usually characteristic of divertor tokamaks, are obvious signature of the complex SOL and are responsible for the high plasma recycling close to the plate.

References

[1] V. Pericoli Ridolfini et al., J. Nucl. Mater. 220–222 (1995) 218.
[2] R. Zagorski, J. Tech. Phys. 37 (1996) 7.
[3] R. Andreani et al., Fusion Technol., Proceedings of the 16th Symposium on Fusion Technology, vol. 1, London, 1990, p. 218.
[4] M. Ciotti, C. Ferro, G. Maddaluno, J. Nucl. Mater. 196–198 (1992) 725.
[5] P.C. Stangeby, G.M. McCracken, Nucl. Fusion 30 (1990) 1225.
[6] M. Leigheb, V. Pericoli Ridolfini, R. Zagorski, J. Nucl. Mater. 241–243 (1997) 914.
[7] S.I. Braginskij, Rev. Plasma Phys. 1 (1996) 205.
[8] H.A. ClaaMen, H. Gerhauser, R.N. Ei-Shavit, Report of KFA Julich, JUL-2423, 1991.
[9] C. Ferro, Characteristic of the FTU scrape-off layer (SOL) determined by a simple l-D model, ENEA Internal Report, RT/ERG/FUS/94/22, 1994.
[10] R. Zanino, C. Ferro, M. Frassinesi, M. Leigheb, these Proceedings.